Magnetic properties of the $S = \frac{1}{2}$ quasisquare lattice antiferromagnet $CuF_2(H_2O)_2(pyz)$ (pyz = pyrazine) investigated by neutron scattering

C. H. Wang,[1] M. D. Lumsden,[1] R. S. Fishman,[1] G. Ehlers,[1] T. Hong,[1] W. Tian,[1] H. Cao,[1] A. Podlesnyak,[1] C. Dunmars,[2] J. A. Schlueter,[2] J. L. Manson,[3] and A. D. Christianson[1]

[1]*Oak Ridge National Laboratory, Oak Ridge, Tennessee 37831, USA*

[2]*Material Science Division, Argonne National Laboratory, Argonne, Illinois 60439, USA*

[3]*Department of Chemistry and Biochemistry, Eastern Washington University, Cheney, Washington 99004, USA*

(Received 23 May 2012; revised manuscript received 4 August 2012; published 27 August 2012)

We have performed elastic and inelastic neutron scattering experiments on single crystal samples of the coordination polymer compound $CuF_2(H_2O)_2(pyz)$ (pyz = pyrazine) to study the magnetic structure and excitations. The elastic neutron diffraction measurements indicate a collinear antiferromagnetic structure with moments oriented along the [0.7 0 1] real-space direction and an ordered moment of $0.60 \pm 0.03\ \mu_B$/Cu. This value is significantly smaller than the single-ion magnetic moment, reflecting the presence of strong quantum fluctuations. The spin wave dispersion from magnetic zone center to the zone boundary points (0.5 1.5 0) and (0.5 0 1.5) can be described by a two-dimensional Heisenberg model with a nearest-neighbor magnetic exchange constant $J_{2D} = 0.934 \pm 0.0025$ meV. The interlayer interaction J_{perp} in this compound is less than 1.5% of J_{2D}. The spin excitation energy at the (0.5 0.5 0.5) zone boundary point is reduced when compared to the (0.5 1 0.5) zone boundary point by $\sim 10.3\% \pm 1.4\%$. This zone boundary dispersion is consistent with quantum Monte Carlo and series expansion calculations for the $S = \frac{1}{2}$ Heisenberg square lattice antiferromagnet, which include corrections for quantum fluctuations to linear spin wave theory.

DOI: 10.1103/PhysRevB.86.064439 PACS number(s): 75.30.Ds, 75.25.−j, 75.50.Ee, 28.20.Cz

I. INTRODUCTION

Metal-organic systems with a $3d^9$ electron configuration, such as in Cu^{2+}, are expected to undergo a Jahn-Teller distortion. In octahedral coordination, this typically elongates one axis of the octahedron and removes the degeneracy of the e_g orbitals $d_{x^2-y^2}$ and d_{z^2}. This effect widely occurs in molecular systems as well as in other materials, such as the colossal magnetoresistance manganites.[1,2] The Jahn-Teller distortion is extremely sensitive to bond distances, and as such, applied pressure can strongly influence or even induce a Jahn-Teller distortion. Depending on the elongation axis in the crystal structure, the pattern of orbital overlaps and related exchange interactions can vary significantly, in turn leading to disparate magnetic ground states. Finding materials where a Jahn-Teller distortion can be tuned to act as a magnetic switch has potential for applications in technological devices and thus is of great interest.

The copper-based coordination polymer magnet $CuF_2(H_2O)_2(pyz)$ (pyz = pyrazine) appears to be a model material for studying the switching of magnetic properties due to changes in the Jahn-Teller axis.[3,4] $CuF_2(H_2O)_2(pyz)$ crystallizes in a monoclinic structure (space group $P2_1/c$) with $a = 7.6926$ Å, $b = 7.5568$ Å, $c = 6.897$ Å, and $\beta = 111.065^\circ$ under ambient conditions.[5,6] The structure consists of $CuF_2O_2N_2$ octahedra, which form a two-dimensional (2D) network in the bc plane. The magnetic susceptibility shows a broad peak at 10.5 K consistent with 2D short-range correlations and three-dimensional long-range order below $T_N = 2.6$ K due to weak coupling along the a axis. At ambient pressure, the Jahn-Teller axis is along the N-Cu-N axis (a direction). Hence the $d_{x^2-y^2}$ magnetic orbital lies in the bc plane to form a 2D antiferromagnetic (AFM) quasisquare lattice where the near-neighbor distances are the same, but the interior angles deviate by about $\pm 5^\circ$. First-principles electronic structure calculations confirm this configuration.[5] These calculations give an intraplane AFM exchange interaction of about 13 to 19 K and an interplane AFM exchange interaction of only 1% of the intraplane exchange interaction. An important feature of $CuF_2(H_2O)_2(pyz)$ is that under an applied pressure of 0.9 GPa, a switch of the Jahn-Teller axis from the N-Cu-N to the O-Cu-O (c direction) bond occurs.[3] When pressure increases to 3.1 GPa, the Jahn-Teller axis switches again from the O-Cu-O bond to the F-Cu-F bond (b direction). Correspondingly, the magnetic interactions are expected to vary at different pressures: from the ambient pressure 2D quasisquare lattice (exchange path Cu-F$\cdots$H-O-Cu) to one-dimensional (1D) chain interactions (exchange path Cu-pyz-Cu) at 0.9 GPa. Indeed, the magnetic susceptibility at ambient pressure can be well described by the 2D Heisenberg square lattice,[5] while above 0.9 GPa the magnetic susceptibility exhibits a broad peak consistent with 1D magnetic correlations.[3] Therefore a microscopic understanding of the magnetic properties at ambient pressure would be an illuminating step towards a complete understanding of the interesting pressure-dependent behavior of $CuF_2(H_2O)_2(pyz)$.

In this paper we present the results of a study of deuterated $CuF_2(H_2O)_2(pyz)$ [$CuF_2(D_2O)_2(d_4\text{-pyz})$] with elastic and inelastic neutron scattering under ambient pressure. The neutron diffraction results show that the sample has a collinear AFM structure with the moments lying in the ac plane along the [0.7 0 1] direction. The spin wave dispersion extracted from the inelastic neutron spectra can be well described by a nearest-neighbor 2D Heisenberg model. The spin wave dispersion found along the interlayer direction could not be observed within the instrumental resolution of FWHM = 0.034 meV. This indicates that the interlayer exchange interaction J_{perp}

is weak, as expected for a 2D system where the spin wave dispersion does not depend on the out-of-plane direction. Consequently, $CuF_2(H_2O)_2(pyz)$ is a good example of a quasi-2D system where the spin wave dispersion depends exclusively on K and L. Within the 2D magnetic plane, the dispersion along the zone boundary points has been measured and is in accord with the prediction of the quantum Monte Carlo and series expansion calculations[7–9] for quantum fluctuation corrections to linear spin wave theory for the $S = \frac{1}{2}$ square lattice Heisenberg antiferromagnet.

II. EXPERIMENTAL DETAILS

In order to minimize attenuation of the beam caused by the large incoherent scattering cross section of hydrogen, fully deuterated $CuF_2(D_2O)_2(d_4\text{-pyz})$ crystals were synthesized for this study. Substitution of deuterium for hydrogen does not alter the crystal symmetry and induces only small changes in the lattice parameters.[6] To ensure that structural parameters of the samples studied here are in accord with previously published values[6] neutron diffraction data (not shown) were collected on the four-circle neutron diffractometer HB-3A at the High Flux Isotope Reactor (HFIR), Oak Ridge National Laboratory. The magnetic structure was studied with the thermal triple-axis spectrometer HB-1 at the HFIR. A crystal with a mass of 0.01 g was studied using HB-3A, while a larger crystal with a mass of 0.1 g was studied with HB-1. A silicon monochromator with no analyzer was used for the measurements on HB-3A, and unless otherwise noted, all triple-axis measurements were performed using pyrolytic graphite (002) monochromator and analyzer crystals.

Inelastic neutron scattering experiments were performed using the cold neutron triple-axis spectrometer CG-4C (HFIR), the thermal triple-axis HB-1A (HFIR), and the cold neutron chopper spectrometer (CNCS)[10] at the Spallation Neutron Source (SNS), Oak Ridge National Laboratory. The inelastic neutron scattering experiments were performed on four coaligned crystals with a total mass of 0.85 g and a total mosaic of 0.7°. For the CG-4C experiment, measurements were made with a fixed final energy E_f of 5 and 3.7 meV, resulting in an elastic energy resolution of about 0.3 and 0.17 meV, respectively. For the HB-1A experiment, the incident energy E_i was fixed at 14.7 meV with a pyrolytic graphite (002) monochromator, and a beryllium (002) analyzer was used to obtain an elastic energy resolution of about 0.58 meV. For the CNCS measurements, the incident energy E_i was fixed at 3 and 1.5 meV to allow examination of the entire spin wave spectrum. The energy resolution (FWHM) was about 0.08 and 0.034 meV at the elastic position for $E_i = 3$ and 1.5 meV, respectively.

III. RESULTS AND DISCUSSION

A. Magnetic structure

Temperature-dependent neutron diffraction reveals the presence of additional peaks for temperatures less than 2.5 K at wave vectors $Q = (0.5\ K\ L)$, with integer values of K and L and where $K + L$ is an odd number. This indicates that in real space the magnetic lattice is doubled along the a direction compared to nuclear lattice, while in the bc plane the nuclear lattice and magnetic lattice remain the same size. Figure 1

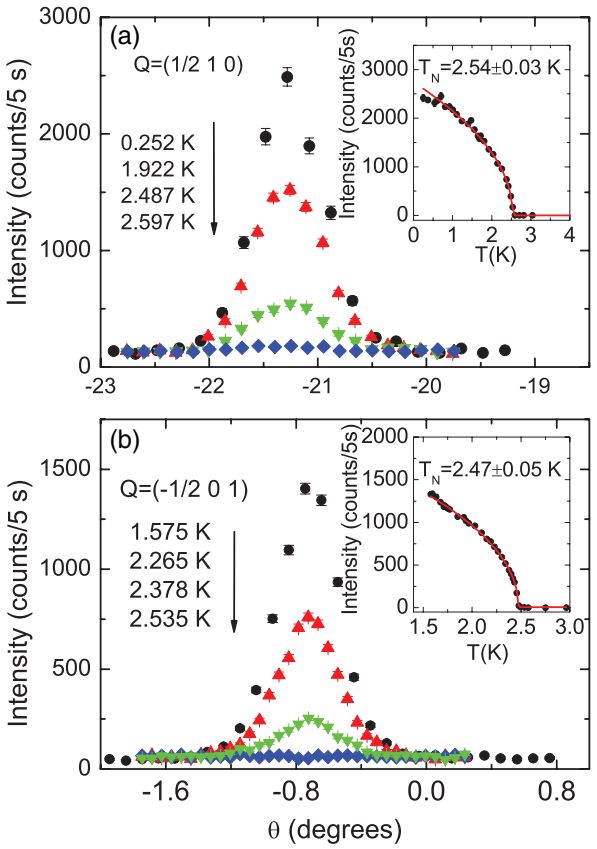

FIG. 1. (Color online) Temperature dependence of magnetic Bragg peaks: (a) (0.5 1 0) and (b) (−0.5 0 1) for $CuF_2(D_2O)_2(d_4\text{-pyz})$. Insets display the temperature-dependent peak intensity. Solid lines are guides to the eye. The data were collected on the HB-1 triple-axis instrument in the $HK0$ and $H0L$ scattering planes, respectively.

shows the temperature-dependent magnetic Bragg peaks at both (0.5 1 0) and (−0.5 0 1) collected on the HB-1 instrument using the final energy $E_f = 13.5$ meV ($\lambda = 2.4617$ Å). In the insets the temperature-dependent peak intensity for (0.5 1 0) and (−0.5 0 1) are presented. A power-law fit of the form $(1 - T/T_N)^{2\beta}$ gives a T_N of 2.51 ± 0.06 K and a value of β of 0.24 ± 0.07. This low value of β is likely consistent with 2D critical behavior; however, care should be used when interpreting this finding as a more rigorous series of measurements is required to definitively establish the critical exponents. The value of T_N determined from the power-law fit is slightly smaller than the value reported by muon spin relaxation measurements of a nondeuterated sample[5,11] but is in reasonable agreement with the value of $T_N = 2.53$ K determined from magnetic susceptibility measurements of fully deuterated samples.[12]

A total of 26 nuclear and 30 magnetic reflections have been collected in the $HK0$ and $H0L$ scattering planes at $T = 0.3$ K using HB-1. Representation analysis for the general case of propagation vector (0.5 0 0) in the structure symmetry $P21/c$ have been performed using SARAh representation analysis.[13] The results show that there are two possible irreducible representations, as shown in Table I. Using the basis vectors in Table I, assuming the magnetic-moment direction $\vec{M} = (M_x\ M_y\ M_z)$

TABLE I. Basis vectors for Cu site 1 [atomic coordinates (0 0 0)] and Cu site 2 [atomic coordinates (0 0.5 0.5)] determined from the representational analysis[13] for space group 14 ($P2_1/c$) and magnetic propagation vector (0.5 0 0). Here IR represents irreducible representations, and BV represents basis vectors.

IR	BV	Cu site 1	Cu site 2
Γ_1	ψ_1	(1 0 0)	(−1 0 0)
	ψ_2	(0 1 0)	(0 1 0)
	ψ_3	(0 0 1)	(0 0 −1)
Γ_3	ψ_4	(1 0 0)	(1 0 0)
	ψ_5	(0 1 0)	(0 −1 0)
	ψ_6	(0 0 1)	(0 0 1)

varies freely, the magnetic reflections can be fitted. For both cases, when $M_y \neq 0$, the spins will configure in a noncollinear way. The fitting of the moment direction was carried out by minimizing

$$\chi^2 = \frac{1}{N}\sum\left[\frac{F_M^{\rm cal}}{F_M^{\rm obs}} - \frac{1}{N}\sum\left(\frac{F_M^{\rm cal}}{F_M^{\rm obs}}\right)\right]^2, \qquad (1)$$

where N is the number of reflections. Fits considering both representations were performed, and the irreducible representation denoted by Γ_1 yielded the best agreement with the data. The resulting collinear spin structure has moments along the [0.7 0 1] real-space direction. For simplicity, the dipole approximation to the Cu^{2+} form factor has been used. This may lead to a systematic error in both the direction and magnitude of the magnetic moment due to the anisotropy of the $d_{x^2-y^2}$ orbital.[14] We note that the Γ_1 irreducible representation with $M_y = 0$ results in an antiparallel alignment of the spins on Cu site 1 [atomic coordinates (0 0 0)] and Cu site 2 [atomic coordinates (0 0.5 0.5)], consistent with the observed propagation vector, which requires $K + L$ to be odd. The resulting magnetic structure for $CuF_2(H_2O)_2$(pyz), shown in Fig. 2, is a G-type (nearest-neighbor) antiferromagnetic order.

Interestingly, the moment direction [0.7 0 1] in real space does not appear to be along an obvious structural direction. The selection of a specific moment direction suggests some anisotropy in the spin Hamiltonian.

The absolute value of the magnetic moment M was determined by comparing the intensity of magnetic and nuclear Bragg reflections. To carefully estimate the moment size, the instrument resolution was taken into account using RESLIB,[15] and the Debye-Waller factor has been included. Our calculations yield an ordered moment of $0.60 \pm 0.03\ \mu_B$/Cu. This value is much smaller than the spin-$\frac{1}{2}$ free-ion moment. In low-dimensional systems a moment reduction occurs due to quantum fluctuations and has been observed in a number of materials.[16,17] The observed and calculated intensities of magnetic and nuclear reflections together with the resulting spin arrangement are presented in Fig. 2.

B. Spin dynamics

The spin wave dispersion has been extracted from inelastic neutron scattering measurements. We first discuss inelastic neutron scattering data collected using the triple-axis spectrometer CG-4C in the $HK0$ scattering plane. Both constant-Q and constant-E scans in the $HK0$ scattering plane have been performed. Constant-E scans at several different energy transfers are plotted in Fig. 3(a), and constant-Q scans are shown in Fig. 3(b). These measurements were carried out along the (0.5 K 0) direction, where $K = 1$ corresponds to the magnetic zone center. The excitation energy at the zone boundary point $Q = (0.5\ 1.5\ 0)$ is $E_{zbK} = 2.24 \pm 0.04$ meV. Within instrumental resolution (FWHM $= 0.17 \pm 0.01$ meV), no energy gap at the antiferromagnetic zone center has been observed.

In Figs. 4(a), 4(b) and 4(c) the spin wave dynamics have been studied with the sample aligned in the $H0L$ scattering plane with the time-of-flight spectrometer CNCS.

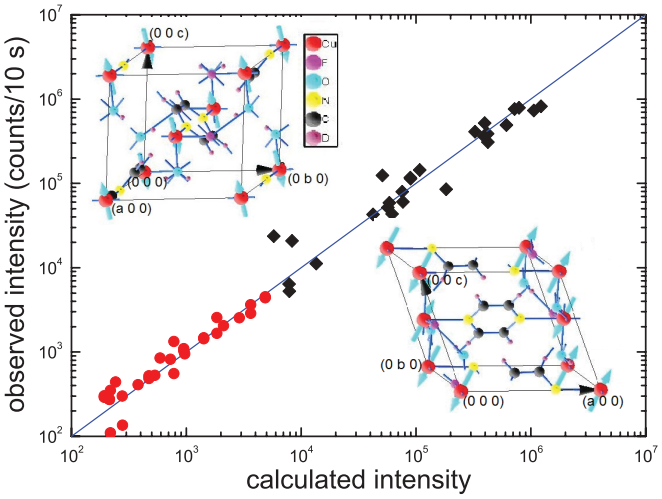

FIG. 2. (Color online) The observed intensity plotted as a function of calculated intensity for $CuF_2(D_2O)_2(d_4$-pyz) at $T = 0.25$ K. Nuclear and magnetic reflections are denoted by diamonds and circles, respectively. The solid line is a guide to the eye. The data were collected on HB-1 in different scattering planes. The insets depict different views of the unit cell. The arrows on Cu atoms indicate the magnetic-moment configuration. The 2D magnetic behavior of $CuF_2(D_2O)_2(d_4$-pyz) originates in the bc plane.

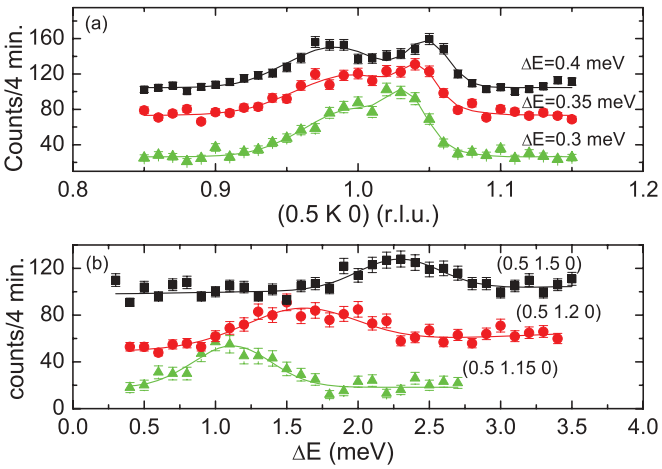

FIG. 3. (Color online) (a) Constant-E scans along (0.5 K 0) collected in the $HK0$ scattering plane at $T = 1.5$ K by the CG-4C spectrometer. (b) Constant-Q scans collected in the $HK0$ scattering plane at $T = 1.5$ K by the CG-4C spectrometer. The solid lines in both panels are fits with Gaussians.

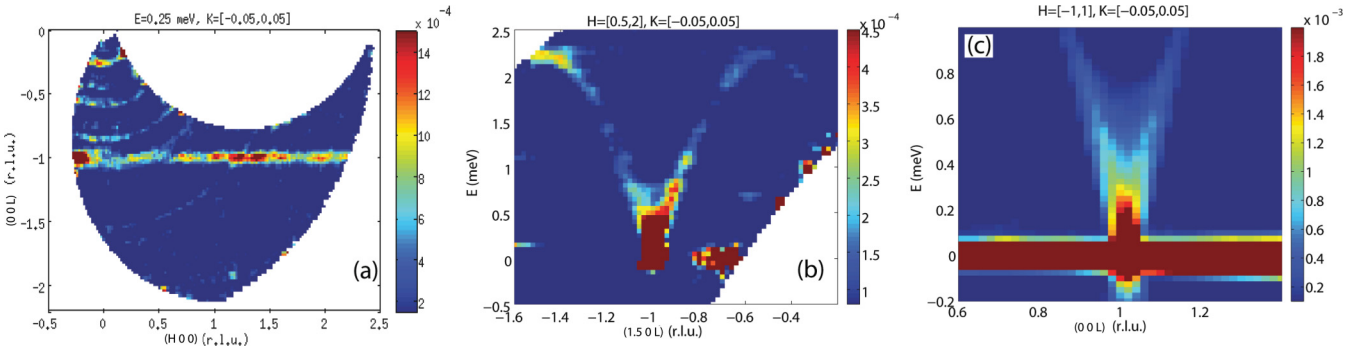

FIG. 4. (Color online) Inelastic neutron scattering data from the time-of-flight spectrometer CNCS. (a) Contour map of intensity in the $H0L$ scattering plane with $\Delta E = 0.25$ meV and $T = 1.5$ K. Background scattering determined from an empty sample holder measurement has been subtracted. (b) The spin wave dispersion along the (1.5 0 L) direction. The data were collected at $T = 1.5$ K, with $E_i = 3$ meV. Background scattering determined from an empty sample holder measurement has been subtracted. (c) Low-energy spin wave dispersion along the (0 0 L) direction in the high-resolution mode at $T = 1.5$ K with $E_i = 1.5$ meV. Intensities in all panels are given in arbitrary units. The integration range is indicated along with the specified direction at the top of each panel. Note that the dispersion was found to be independent of the value of H, and as such the integration range over H was chosen to be large to increase statistics.

Figure 4(a) shows that the spin wave excitation is essentially independent of H at the excitation energy $\Delta E = 0.25$ meV, implying only weak interactions along H. In Fig. 4(b), the full dispersion along the L direction is shown. The zone boundary energy in this direction is $E_{\mathrm{zbL}} = 2.204 \pm 0.003$ meV. This value is consistent with the previously determined zone boundary energy along the K direction ($E_{\mathrm{zb}K}$). To search for a small energy gap, measurements were performed on CNCS using an incident energy of 1.5 meV, resulting in an energy resolution of FWHM $= 0.034 \pm 0.0007$ meV). The measurements were centered on the (0.5 0 1) magnetic zone center. The data obtained along the L direction are shown in Fig. 4(c). Again, within instrumental resolution (FWHM $=$ 0.034 meV), no energy gap in the L dispersion curve was observed. Furthermore, no dispersion was observed along the H direction for $L = 1$. We note that previous DFT calculations predict an interlayer exchange constant of 0.011 meV (Ref. 5), and the resulting interlayer dispersion could not be observed with our instrumental resolution. Nearly identical exchange interactions along the K and L directions together with the lack of dispersion along the H direction indicates the magnetism in $CuF_2(D_2O)_2(d_4\text{-pyz})$ is predominately 2D.

The interlayer H-direction magnetic exchange was also probed with time-of-flight spectrometer CNCS in a high-resolution mode with $E_i = 1.5$ meV. The H vs E slice for $L = 1$ (not shown here) is featureless, and no obvious spin excitation has been observed within instrument resolution. Due to the fact that in spin wave theory the zone boundary energy of the spin wave excitation is of order $2J$, our data show that the interlayer exchange interaction J_{perp} is expected to be smaller than $\frac{0.034}{2}$ meV $= 0.017$ meV. Considering $E_{\mathrm{zbL}} = 2.204$ meV, which gives an intralayer J of 1.102 meV, it is reasonable to estimate that the interlayer exchange interaction is less than 1.5% of the intralayer exchange interaction. This ratio is in agreement with that determined by both DFT calculations and by fitting a Heisenberg square lattice model to the magnetic susceptibility, which in both cases yields $J_{\mathrm{perp}}/J_{2D} \sim 1\%$.[5]

Since no energy gap has been observed in the 2D square lattice plane at the magnetic zone center within instrumental resolution, it is reasonable to believe that any spin exchange anisotropy must be very small. However, the magnetic moments select the [0.7 0 1] direction, suggesting nevertheless that a spin anisotropy is present. As Cu^{2+} moments should have no single-ion anisotropy and the presence of inversion symmetry prohibits Dzyaloshinskii-Moriya interactions, we have included exchange anisotropy of the following form:

$$\hat{H} = J \sum \left[S_i^z S_j^z + \Delta \left(S_i^x S_j^x + S_i^y S_j^y \right) \right], \tag{2}$$

where the summation is over the nearest neighbors in the 2D plane, J is the effective intralayer exchange parameter, and Δ is the exchange anisotropy parameter.

Linear spin wave theory yields the spin wave dispersion,

$$\hbar\omega_Q = 2J\sqrt{1 - \Delta^2 \cos^2(K\pi)\cos^2(L\pi)}, \tag{3}$$

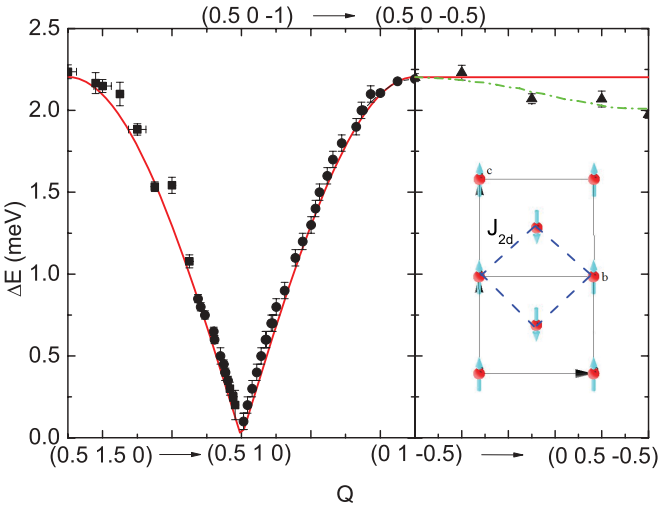

FIG. 5. (Color online) Summary of the spin wave dispersion for $CuF_2(D_2O)_2(d_4\text{-pyz})$. The data were collected using CNCS (solid circles), CG-4C (solid squares), and HB-1A (solid triangles). The solid line represents the dispersion of the Heisenberg linear spin wave theory with a nearest-neighbor interaction. The dash-dotted line represents the results of series expansion to higher order.[8] The inset depicts the bc plane. The dashed lines show the square lattice with a nearest-neighbor exchange interaction.

where Q is a function of K and L. The dashed lines in the inset of Fig. 5 indicate the diamond pattern on which the Cu ions are positioned. Under the approximation that the diamond is replaced by a square, the abscissa labels in Fig. 5 are related to square lattice notation in the following way: (0.5 1 0) and (0.5 0 1) correspond to $(\pi\,\pi)$, (0.5 1.5 0) and (0.5 0 1.5) correspond to $(\pi/2\ \pi/2)$, and, finally, the point (0 0.5 −0.5) corresponds to $(\pi\ 0)$. In Fig. 5 we plot the extracted dispersion relation for $CuF_2(D_2O)_2(d_4\text{-pyz})$. The experimental data in the 2D plane were determined from combinations of triple-axis and time-of-flight measurements. The solid line in Fig. 5 is the expected dispersion behavior of the classical Heisenberg model ($\Delta = 1$) with $J = 1.102 \pm 0.003$ meV.

In the $S = \frac{1}{2}$ Heisenberg square lattice antiferromagnet, it is well established that the spin dynamics can be well described by the classical linear spin wave theory with the inclusion of quantum corrections.[7–9,18–20] The net effect of quantum corrections is an overall renormalization factor, $Z_c \approx 1.18$, resulting in an effective coupling constant $J_{\text{eff}} = Z_c J_{2D}$ when considering the dispersion from the $(\pi\ \pi)$ zone center to the $(\pi/2\ \pi/2)$ zone boundary. Thus, our extracted exchange constant, J, is an effective coupling constant, and the resulting J_{2D} is 0.934 ± 0.0025 meV within the square lattice approximation. This value is consistent with estimates from the magnetic susceptibility and magnetization measurements of fully deuterated samples where J_{2D} is about 0.94 meV.[12]

The dispersion resulting from the anisotropic exchange yields a zone center energy gap of $E_{zc} = 2J\sqrt{1-\Delta^2}$. As noted previously, we have not observed such a gap within the instrumental resolution of 0.034 meV. This allows us to place a lower bound on Δ. The coupling constant extracted from the zone boundary measurements is $J = 1.102 \pm 0.003$ meV. Placing an upper bound on the gap energy of 0.034 meV results in a value of Δ (the ratio J_{xy}/J_z) of at least 0.99988. The result would be a very small anisotropy resulting in a slightly larger J_z, which would favor a spin orientation along the z axis. Note that the z axis is the spin wave quantization direction, in this case the real-space [0.7 0 1] direction. This same spin anisotropy may be related to the observed low-field spin-flop-like transition observed for $CuF_2(H_2O)_2(pyz)$.[5]

The spin wave dispersion has been examined along the antiferromagnetic zone boundary. In Fig. 6 we present constant-Q scans along $(0\ K\ -0.5)$ from $K = 1$ [square lattice $(\pi/2\ \pi/2)$] to $K = 0.5$ [square lattice $(\pi\ 0)$]. In Fig. 5 the observed dispersion between (0 1 −0.5) and (0 0.5 −0.5) has been plotted. Compared to (0 1 −0.5), the excitation energy at (0 0.5 −0.5) has been suppressed by 10.3% ± 1.4%. This observation is inconsistent with linear spin wave theory, where there is no dispersion along the zone boundary. However, proper inclusion of quantum fluctuations using series expansion and quantum Monte Carlo techniques for the $S = \frac{1}{2}$ 2D AFM square lattice predict a dispersion along the zone boundary with the energy at $(\pi\ 0)$ 7%–10% lower than that at $(\pi/2\ \pi/2)$.[7–9] Experimental behavior consistent with these calculations has been seen in several model systems.[16,21–23] However, there are some materials where conflicting experimental observations exist. For instance, in La_2CuO_4 (Ref. 23) the energy scale at $(\pi\ 0)$ is about 7% larger than the value at $(\pi/2\ \pi/2)$, in contrast to the expected quantum behavior, which has been attributed to

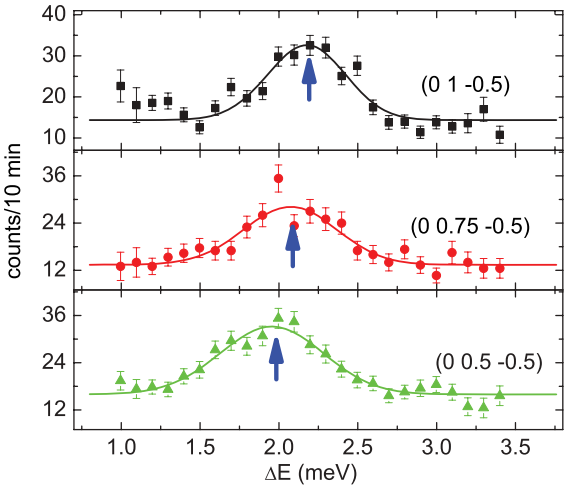

FIG. 6. (Color online) Constant-Q scans along the zone boundary points ranging from (0 1 −0.5) to (0 0.5 −0.5). The solid line are fits to a Gaussian. The data were collected on HB-1A.

ring exchange among four spins in the CuO_2 plane. In the coordination polymer compound $Cu(pyz)_2(ClO_4)_2$,[16] the excitation energy at $(\pi\ 0)$ is reduced by 11.5% compared to the energy at $(\pi/2\ \pi/2)$. The authors believe this value is larger than the expectation of series expansion and quantum Monte Carlo calculations, and they attribute this stronger suppression to the next-nearest-neighbor interactions, which enhance quantum fluctuations. In $K_2V_3O_8$ (Ref. 17) a striking feature of two modes near the zone boundary point $(\pi/2\ \pi/2)$ has been observed experimentally, and no fully satisfactory explanation has yet been given for this behavior. For our measurements on $CuF_2(D_2O)_2(d_4\text{-pyz})$, in Fig. 5 the dash-dotted line is the results of calculations including quantum fluctuations with nearest-neighbor interactions.[8] It is clear that the data points follow the expected theory, and therefore we interpret the zone boundary dispersion behavior in $CuF_2(D_2O)_2(d_4\text{-pyz})$ as being consistent with the $S = \frac{1}{2}$ near-neighbor 2D AFM square lattice with inclusion of quantum corrections.

IV. CONCLUSION

We have performed a series of elastic and inelastic neutron scattering experiments to study the 2D spin-$\frac{1}{2}$ quasisquare lattice antiferromagnet $CuF_2(D_2O)_2(d_4\text{-pyz})$. The 2D magnetic lattice in the bc plane is the same size as the nuclear structure lattice, while along the a direction the magnetic lattice is doubled. The ordered magnetic moment of the Cu^{2+} ions is found to be $0.60 \pm 0.03\ \mu_B$, which is significantly reduced from the expected $1\ \mu_B$, indicating strong quantum fluctuations. The spins adopt a collinear antiferromagnetic alignment for nearest-neighbor sites in the 2D plane and are oriented along the real-space [0.7 0 1] direction.

The spin dynamics of $CuF_2(D_2O)_2(d_4\text{-pyz})$ have been studied using inelastic neutron scattering data obtained from both triple-axis and time-of-flight instruments. The 2D spin wave dispersion can be described by a nearly isotropic spin Hamiltonian with small nearest-neighbor interaction

$J_{2D} = 0.934 \pm 0.0025$ meV and very weak interlayer coupling. Along the magnetic zone boundary, the excitation energy shows a 10.3% $\pm$ 1.4% dispersion consistent with square lattice calculations, including quantum fluctuations.

ACKNOWLEDGMENTS

Research work at ORNL was sponsored by the Laboratory Directed Research and Development Program of ORNL and was supported by the Scientific User Facilities Division, Office of Basic Energy Sciences, DOE. This research was sponsored by the Division of Materials Science and Engineering of the US Department of Energy (R.S.F.). This work was supported by UChicago Argonne, LLC, operator of Argonne National Laboratory (Argonne). Argonne, a US Department of Energy Office of Science laboratory, is operated under Contract No. DE-AC02-06CH11357. Work at EWU was supported by the NSF under Grant No. DMR-1005825.

[1] M. Capone, M. Fabrizio, C. Castellani, and E. Tosatti, Rev. Mod. Phys. **81**, 943 (2009).
[2] M. B. Salamon and M. Jaime, Rev. Mod. Phys. **73**, 583 (2001).
[3] G. J. Halder, K. W. Chapman, J. A. Schlueter, and J. L. Manson, Angew. Chem., Int. Ed. Engl. **50**, 419 (2011).
[4] A. Prescimone, C. Morien, D. Allan, J. Schlueter, S. Tozer, J. L. Manson, S. Parsons, E. K. Brechin, and S. Hill, Angew. Chem., Int. Ed. Engl. **51**, 7490 (2012).
[5] J. L. Manson, M. M. Conner, J. A. Schlueter, A. C. McConnell, H. I. Southerland, I. Malfant, T. Lancaster, S. J. Blundell, M. L. Brooks, F. L. Pratt, J. Singleton, R. D. McDonald, C. Lee, and M.-H. Whangbo, Chem. Mater. **20**, 7408 (2008).
[6] J. A. Schlueter, H. Park, J. L. Manson, H. Nakotte, and A. J. Schultz, Phys. B **405**, S324 (2010).
[7] R. R. P. Singh and M. P. Gelfand, Phys. Rev. B **52**, R15695 (1995).
[8] W. Zheng, J. Oitmaa, and C. J. Hamer, Phys. Rev. B **71**, 184440 (2005).
[9] A. W. Sandvik and R. R. P. Singh, Phys. Rev. Lett. **86**, 528 (2001).
[10] G. Ehlers, A. A. Podlesnyak, J. L. Niedziela, E. B. Iverson, and P. E. Sokol, Rev. Sci. Instrum. **82**, 085108 (2011).
[11] P. A. Goddard, J. Singleton, P. Sengupta, R. D. McDonald, T. Lancaster, S. J. Blundell, F. L. Pratt, S. Cox, N. Harrison, J. L. Manson, H. I. Southerland, and J. A. Schlueter, New J. Phys. **10**, 083025 (2008).
[12] P. A. Goddard, J. Singleton, C. Maitland, S. J. Blundell, T. Lancaster, P. J. Baker, R. D. McDonald, S. Cox, P. Sengupta, J. L. Manson, K. A. Funk, and J. A. Schlueter, Phys. Rev. B **78**, 052408 (2008).
[13] A. S. Wills, Phys. B **276**, 680 (2000).
[14] I. A. Zaliznyak and S.-H. Lee, in *Modern Techniques for Characterizing Magnetic Materials*, edited by Y. Zhu (Kluwer Academic, Boston, 2005), pp. 22–24.
[15] A. Zheludev, Triple-axis resolution library for MATLAB, http://neutron.ornl.gov/zhelud/reslib/.
[16] N. Tsyrulin, T. Pardini, R. R. P. Singh, F. Xiao, P. Link, A. Schneidewind, A. Hiess, C. P. Landee, M. M. Turnbull, and M. Kenzelmann, Phys. Rev. Lett. **102**, 197201 (2009); N. Tsyrulin, F. Xiao, A. Schneidewind, P. Link, H. M. Rønnow, J. Gavilano, C. P. Landee, M. M. Turnbull, and M. Kenzelmann, Phys. Rev. B **81**, 134409 (2010).
[17] M. D. Lumsden, S. E. Nagler, B. C. Sales, D. A. Tennant, D. F. McMorrow, S.-H. Lee, and S. Park, Phys. Rev. B **74**, 214424 (2006).
[18] R. R. P. Singh, Phys. Rev. B **39**, 9760 (1989).
[19] J. I. Igarashi, Phys. Rev. B **46**, 10763 (1992).
[20] C. M. Canali, S. M. Girvin, and M. Wallin, Phys. Rev. B **45**, 10131 (1992).
[21] Y. J. Kim, A. Aharony, R. J. Birgeneau, F. C. Chou, O. Entin-Wohlman, R. W. Erwin, M. Greven, A. B. Harris, M. A. Kastner, I. Ya. Korenblit, Y. S. Lee, and G. Shirane, Phys. Rev. Lett. **83**, 852 (1999).
[22] H. M. Rønnow, D. F. McMorrow, R. Coldea, A. Harrison, I. D. Youngson, T. G. Perring, G. Aeppli, O. Syljuåsen, K. Lefmann, and C. Rischel, Phys. Rev. Lett. **87**, 037202 (2001).
[23] R. Coldea, S. M. Hayden, G. Aeppli, T. G. Perring, C. D. Frost, T. E. Mason, S.-W. Cheong, and Z. Fisk, Phys. Rev. Lett. **86**, 5377 (2001).